

Review

Catalytically Active Advanced Two-Dimensional Ultrathin Nanomaterials for Sustainable Energy

FuJie Liu ¹, Chao Wang ², Ming Zhang ^{2,*}  and Mengxia Ji ^{2,*} 

¹ Zhenjiang Key Laboratory of Functional Chemistry, Institute of Medicine and Chemical Engineering, Zhenjiang College, 518 Changxiang West Avenue, Zhenjiang 212028, China

² Institute for Energy Research, School of the Environment and Safety Engineering, Jiangsu University, 301 Xuefu Road, Zhenjiang 212013, China

* Correspondence: zm@ujs.edu.cn (M.Z.); jmx@ujs.edu.cn (M.J.); Tel./Fax: +86-0511-88791108 (M.Z. & M.J.)

Abstract: Advanced two-dimensional (2D) ultrathin nanomaterials' unique structural and electronic properties and their applications in the photo-, photoelectro-, and electro-catalysis fields present timely topics related to the development of sustainable energy. This critical review briefly summarizes the state-of-the-art progress on 2D ultrathin nanomaterials. In this mini review, we started with the synthesis of 2D ultrathin nanomaterials. Then, various strategies for tailoring the electronic and configuration structures of these nanomaterials in the new energy catalysis field are surveyed, where the emphasis is mainly on structure-activity relationships. The advancements of versatile 2D ultrathin nanomaterials in the fields of hydrogen evolution, carbon dioxide conversion, and dinitrogen fixation for sustainable energy were also discussed. Finally, the existing challenges and future research directions in this promising field are presented.

Keywords: two-dimensional materials; ultrathin structure; catalysis; sustainable energy



Citation: Liu, F.; Wang, C.; Zhang, M.; Ji, M. Catalytically Active Advanced Two-Dimensional Ultrathin Nanomaterials for Sustainable Energy. *Catalysts* **2022**, *12*, 1167. <https://doi.org/10.3390/catal12101167>

Academic Editor: Bin Luo

Received: 5 September 2022

Accepted: 29 September 2022

Published: 3 October 2022

Publisher's Note: MDPI stays neutral with regard to jurisdictional claims in published maps and institutional affiliations.



Copyright: © 2022 by the authors. Licensee MDPI, Basel, Switzerland. This article is an open access article distributed under the terms and conditions of the Creative Commons Attribution (CC BY) license (<https://creativecommons.org/licenses/by/4.0/>).

1. Introduction

With the increasing consumption of fossil fuels and the expediting process of industrialization in recent decades, the aggravated environmental damage and energy problems have forced the urgent need to develop sustainable and green energy [1–3]. Photo/electrochemical energy conversion technology, including hydrogen evolution from water splitting, carbon dioxide conversion, and dinitrogen fixation, etc. is considered to be a practical measure for renewable fuel generation with the merits of mild, economical, and low-emission characteristics [4–8]. However, the sluggish redox kinetics of the photo/electrocatalytic systems leads to a suboptimal total energy conversion efficiency, especially from further industrial-scale applications. As a consequence, the reasonable design of highly efficient catalysts is of great importance to enhance the overall performance.

The groundbreaking work on graphene in 2004 indicates that enormous efforts have been devoted to exploring the two-dimensional (2D) ultrathin nanomaterial [9]. The nanomaterials of this type are a feature of the atomic thickness (typically less than 5 nm), which has attracted extensive research interest in the fields of optoelectronics, catalysis, and energy storage [10–12]. When reducing the thickness of 2D bulk materials to the single or few atoms scale, the local atomic structure will change, including bond angle, bond length, coordination number, and surface atom disorder degree. Furthermore, thanks to the ultrathin structures, drastic increased specific surface area, mechanical flexibility, charge migration rate, and intrinsic quantum confinement effect make 2D ultrathin nanomaterials exhibit diversified physical and chemical properties [13]. For example, the interfacial electron transfer resistance in electrochemistry would be greatly decreased via strengthening the close contact with the electrode substrate due to the flexible feature of 2D ultrathin nanomaterials. Besides, high transport mobility of the in-plane electrons would favor an expeditious electron migration process, thus boosting the electrocatalytic activity. On

the other hand, highly exposed reactive sites arising from the high specific surface area ensure sufficient adsorption and activation centers for substrate molecules. The large surface-to-volume ratio also favors the elevated solar light capture ability and charge carrier migration and transfer rates from the interior to the surface. Meanwhile, the plentiful coordination-unsaturated atoms of ultrathin nanosheets could serve as surface-active sites as well, which induces the enhanced catalytic activity. In previous reported literatures, Sun et al. exhaustively summarized the characterizations on the factors affecting the active sites of 2D ultrathin materials, including the techniques of X-ray absorption fine structure spectroscopy, high-resolution transmission electron microscope, positron annihilation spectroscopy, and electron spin resonance [14]. In addition to 2D materials, single-atom catalysts have gradually become an emerging frontier in the field of catalysis. Wang et al. focused on the concept of a new category of catalysts with the integration of 2D materials and single-atom catalysts for catalysis applications [15]. Consequently, 2D nanomaterials with an ultrathin thickness are one of the most potential candidates for fabricating highly efficient energy conversion systems, as presented in Figure 1. A review on the steerable fabrication of 2D ultrathin nanomaterials and their activity optimization strategies for the energy-related photo/electrochemical applications is highly desired to impel the leap-forward development of this emerging field.

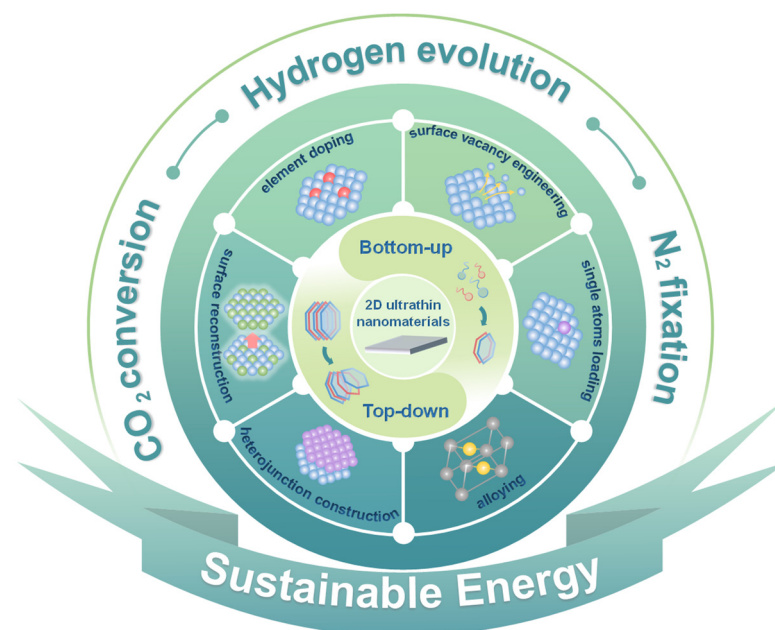


Figure 1. Schematic overview of 2D ultrathin nanomaterials topics covered in this review, including the fabrication approaches, modification strategies, and sustainable energy applications.

In this mini review, we briefly summarize the top-down approaches and bottom-up approaches for the synthesis of 2D ultrathin nanomaterials. In addition, several modification strategies for tuning the catalytic performance in the applications for new energy catalysis are also discussed. Furthermore, the existing challenges and future research directions in this promising field are also presented.

2. The Synthesis of 2D Ultrathin Nanomaterials

A principal classification of 2D ultrathin nanomaterials for photo/electrochemical energy catalysis can be classified as the following types: layered double hydroxides (LDH), transition metal dichalcogenides (TMDCs), transition metal phosphides (TMPs), metal-organic frameworks (MOFs), metal carbides and nitrides (MXenes), oxyhalides, metal-free catalysts, and others [16–21]. Broad attention has been paid to exploring the universal strategies for the preparation of high-quality 2D ultrathin nanosheet materials. Generally,

the most frequently used synthetic methods include physical vapor deposition (PVD), chemical vapor deposition (CVD), liquid/gas exfoliation, surfactant self-assembly, mechanical cleavage, template-directing, chemical etching, etc.

PVD synthesis, with the advantage of low power consumption, high throughput, thickness uniformity, and repeatability, has inherent qualities in the large-scale processing of van der Waals materials. Zhou et al. used the PVD method under atmospheric pressure to grow high-quality monolayered α - In_2Se_3 on the SiO_2/Si substrate in a short amount of time, heating the In_2Se_3 powder to $850\text{ }^\circ\text{C}$ in 30 min (Figure 2a) [22]. However, harsh requirements for the synthetic temperature, type of nanomaterials, and experimental environment limit the application scenarios of the PVD method, even for large-scale applications. Apart from the top-down approach of PVD, the CVD method is also regarded as an effective bottom-up approach for the preparation of high-quality ultrathin nanomaterials, such as MoTe_2 , MoS_2 , CdS , and so on [23–25]. Similarly, the low catalyst yield and specific fabrication requirements also greatly weakened the application potential of CVD technology in the preparation of non-layered 2D ultrathin materials. In addition to the PVD method, mechanical cleavage, chemical etching, and liquid/gas exfoliation methods are the other approaches for the exfoliation of bulk materials with interlayer van der Waals force. Lukowski et al. reported metallic WS_2 nanosheets via facile chemical exfoliation from WS_2 nanostructures synthesized by CVD, including a simple and fast microwave-assisted intercalation reaction method [26]. Yang et al. chose isopropanol as the dispersion medium to produce few-layered carbon nitride nanosheets with a thickness of around 2 nm via a simple liquid phase exfoliation (Figure 2b) [27]. Except for the graphitic carbon nitride, a series of catalysts such as black phosphorus and molybdenum disulfide established that the liquid exfoliation process had the merits of facile control, environment-friendliness, and an easy scale-up. However, extremely low yields of monolayers severely restricted the application of the liquid exfoliation method. Recently, Zhu et al. strove for an efficient and scalable synthesis of ultrathin hexagonal boron nitride nanosheets via a combination of high temperature gas exfoliation and cryogenic liquid nitrogen gasification (Figure 2c) [28]. The thickness of the obtained ultrathin boron nitride nanosheets mainly centered around 1–5 layers after 10 repeated cycles, and the yield could be maintained at 16–20% by weight. This novel thermal expansion triggered gas exfoliation method effectively improved the defects of liquid phase exfoliation.

Differing from the bulk materials with interlayer van der Waals force, it is difficult to directly obtain the ultrathin nanosheet structure of the non-layered structural materials through top-down approaches due to the anisotropy of crystal growth. Hence, bottom-up strategies have been put forward for the fabrication of 2D ultrathin nanosheets by assembling small building blocks, such as self-assembly strategies, template-based approaches, and surfactant self-assembly strategies, etc. [29–32]. These strategies are more controllable, more uniform, and higher yield, showing broader prospects of material preparation. According to a “template-assisted oriented growth” strategy, Cheng and his co-workers created freestanding transition-metal oxide α - Fe_2O_3 nanosheets with a half-unit-cell thickness, as displayed in Figure 3 [33]. During the synthesis process, CuO nanoplate served as the base template for the growth of Fe hydroxide nanosheets. After the template etching treatment, the half-unit-cell α - Fe_2O_3 nanosheets could be achieved by further heating treated dehydrogenation. The surfactant self-assembly approach was regarded as another important strategy for building 2D ultrathin nanomaterials. The monolayer Bi_2WO_6 could be configured in two ways: sandwich substructure ($[\text{BiO}]^+ - [\text{WO}_4]^{2-} - [\text{BiO}]^+$) and non-sandwich substructure ($[\text{Bi}_2\text{O}_2]^{2+} - [\text{WO}_4]^{2-}$). Zhou et al. developed a cetyltrimethylammonium bromide (CTAB)-assisted bottom-up route for the fabrication of monolayer Aurivillius oxide Bi_2WO_6 photocatalyst with a sandwich substructure (Figure 4) [34]. The Br^- ions from CTAB firmly bonded to the monolayer surface, making the surface negatively charged. Furthermore, the stack of monolayers was impeded by the hydrophobic chains of CTA^+ ions and Coulomb repulsion forces. Moreover, our group reported a facile polyvinyl pyrrolidone (PVP) surfactant-assisted solvothermal method for the controllable formation

of a series of bismuth oxyhalide (BiOX , $X = \text{Cl, Br, I}$) nanosheets with atomic level thickness [35–38]. Thanks to the repulsive force among polyvinyl groups, the passivation layers around BiOX hamper the crystal growth along the c -axis, so the ultrathin structure could be obtained. According to these targeted preparation strategies, assorted nanomaterials with ultrathin, even single-layer structures, are achievable to be further synthesized.

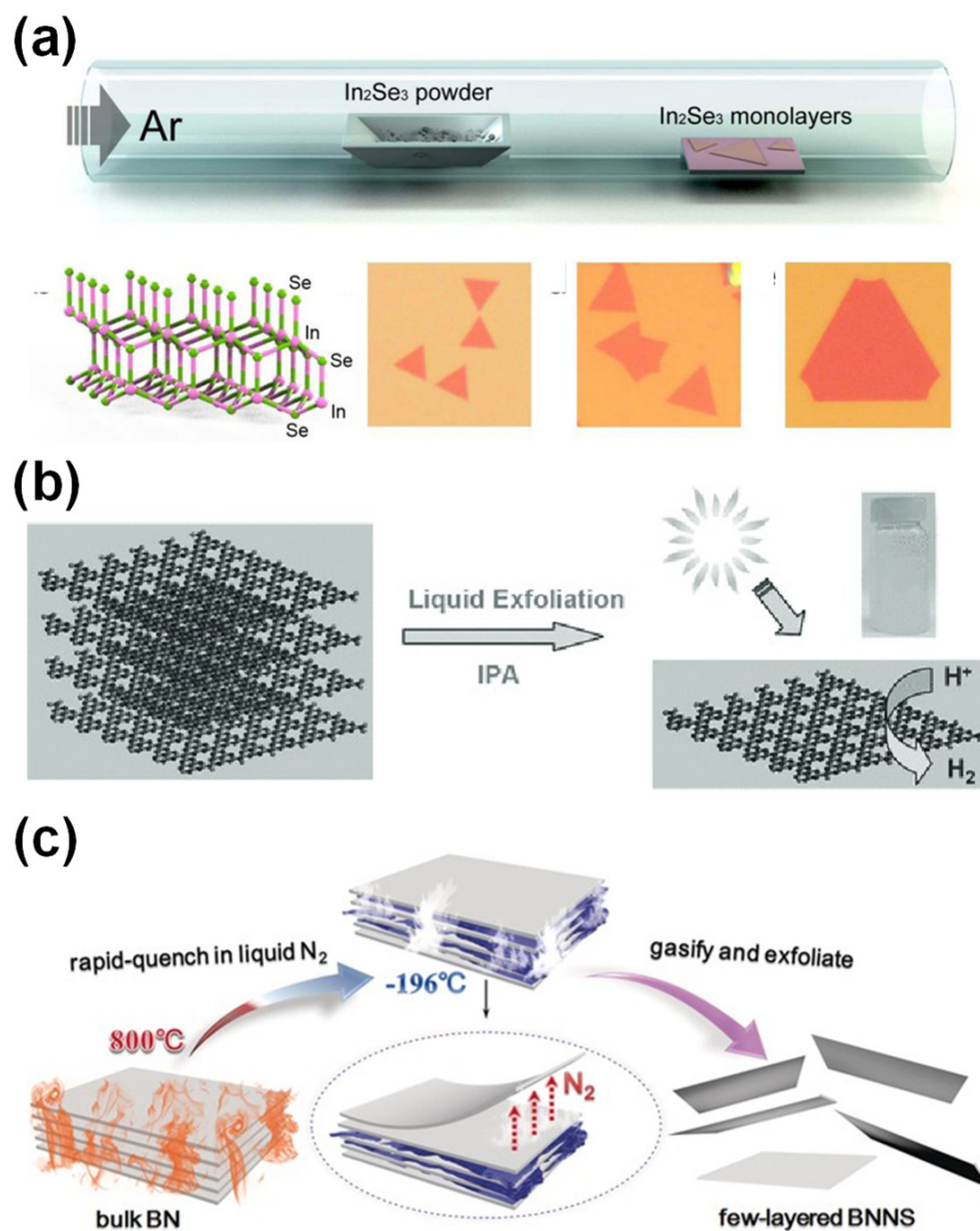


Figure 2. Several top-down approaches for the synthesis of 2D ultrathin nanomaterials: (a) Growth of atomic layered In_2Se_3 via a PVD method and the corresponding optical images [22]. Copyright 2015, American Chemical Society; (b) Synthesis of $\text{g-C}_3\text{N}_4$ ultrathin nanosheets via liquid phase exfoliation from bulk $\text{g-C}_3\text{N}_4$ [27]. Copyright 2013, Wiley-VCH; (c) Gas exfoliation of hexagonal boron nitride ultrathin nanosheets triggered by thermal expansion [28]. Copyright 2016, Wiley-VCH.

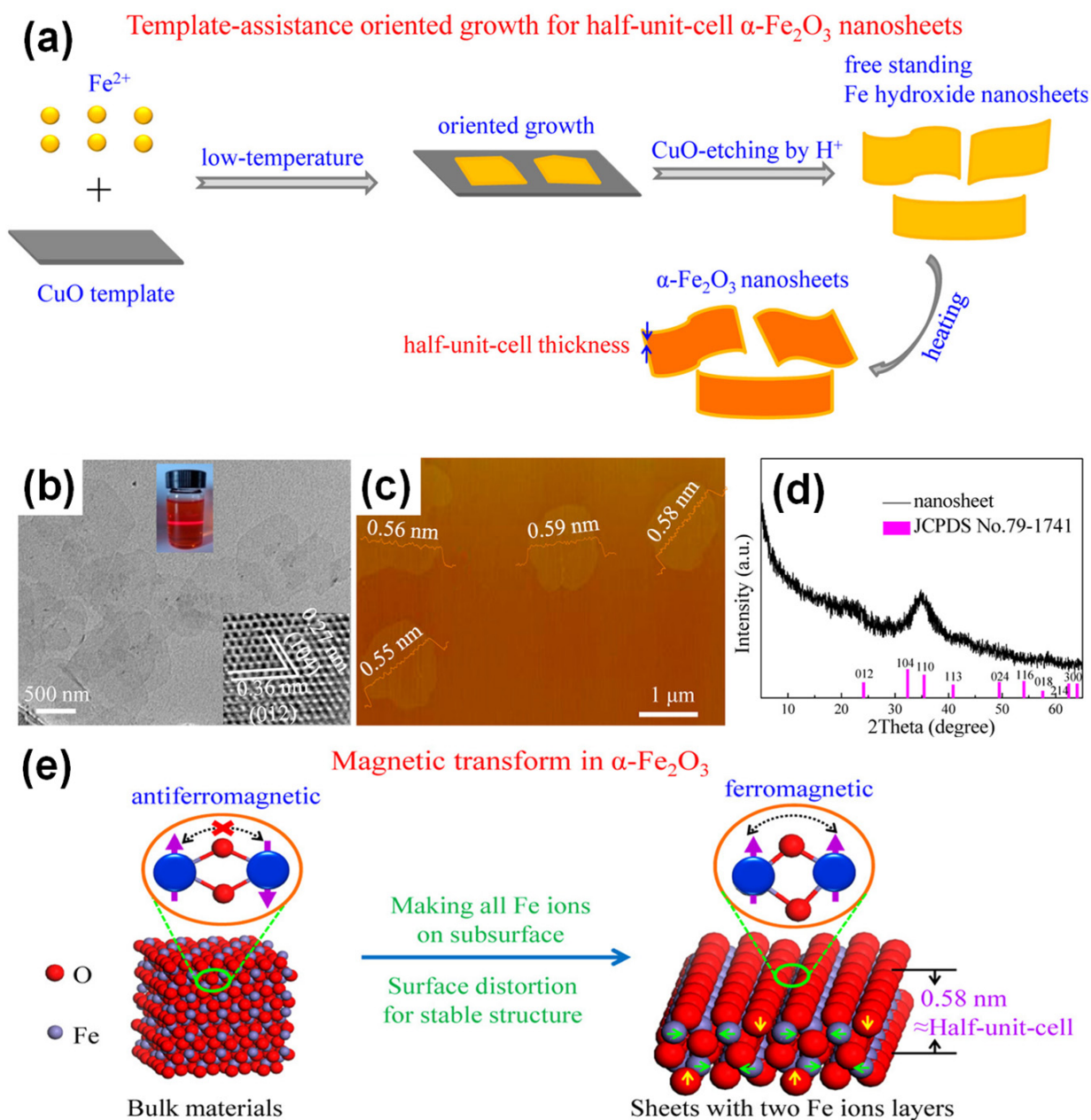


Figure 3. (a) Schematic of preparation process of the half-unit-cell $\alpha\text{-Fe}_2\text{O}_3$ nanosheets; (b) TEM image, (c) AFM image (d), XRD pattern of the $\alpha\text{-Fe}_2\text{O}_3$ nanosheets; (e) Schematic magnetic interaction turnover model for the $\alpha\text{-Fe}_2\text{O}_3$ nanosheets [33]. Copyright 2014, American Chemical Society.

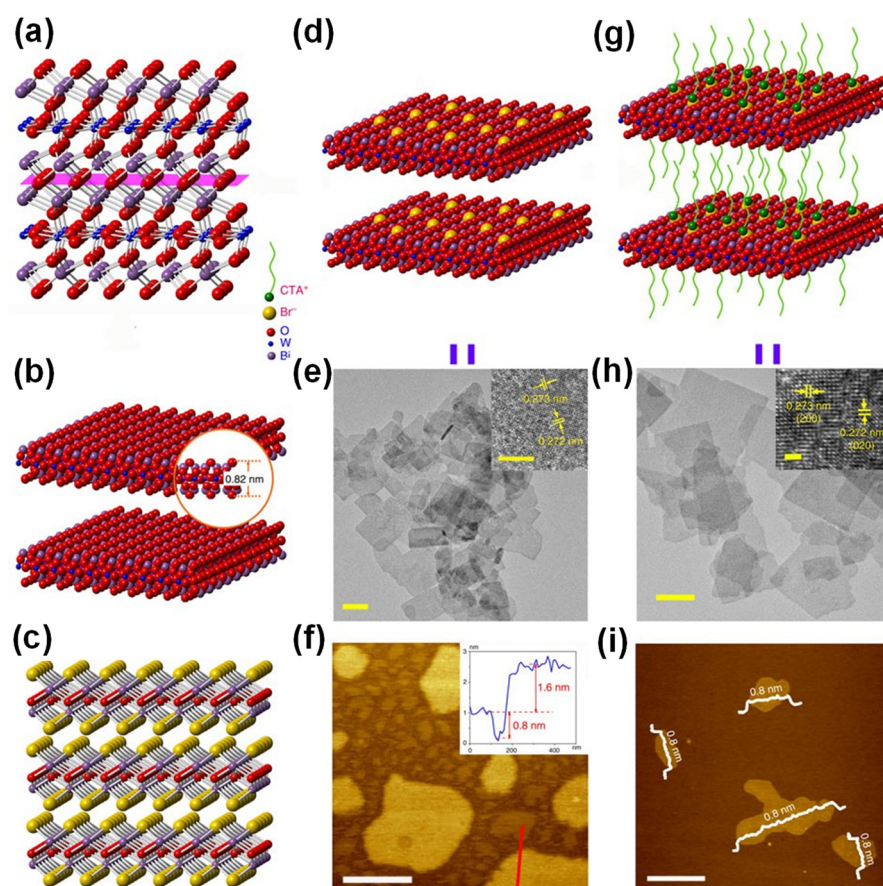


Figure 4. (a) Crystal structure of Bi_2WO_6 ; (b) Structure of pristine monolayer Bi_2WO_6 ; (c) Crystal structure of BiOBr ; (d) Formation mechanism of the monolayer Bi_2WO_6 with Br^- ions assistance; (e) TEM and (f) AFM image of the Bi_2WO_6 nanosheets with Br^- ions assistance, respectively; (g) Growth mechanism of the monolayer Bi_2WO_6 photocatalyst with CTAB assistance; (h) TEM and (i) AFM image of the monolayer Bi_2WO_6 photocatalyst with CTAB assistance. Scale bar, 500 nm (f,i), 50 nm (e,h), 5 nm (insets in (e)) and 1 nm (insets in (h)) [34]. Copyright 2015, Nature Publishing Group.

3. Regulations on Ultrathin Nanomaterials for Energy Catalysis

2D ultrathin nanomaterials have attracted growing attention in sustainable energy development for their exceptional features of captivating electrical conductivity, large surface area, and high mechanical flexibility. To further enhance the catalytic activities for sustainable energy production, various strategies such as surface modification, vacancy engineering, alloying, heterojunction, elements doping, and single atoms anchoring have been adopted to modulate the optical, electronic, and chemical characteristics of 2D ultrathin nanosheet materials [39–43].

Directly converting CO_2 molecules into high value-added fuels and chemical feedstock by using sustainable solar energy and renewable electricity is a promising clean approach to address the energy crisis and greenhouse effect. However, the extremely high thermodynamic stability and $\text{C}=\text{O}$ bond dissociation energy (>750 kJ/mol) of the CO_2 molecule seriously limits the conversion efficiency and selectivity for the vast majority of bulk materials. 2D ultrathin structural catalysts have aroused a growing interest for their unique surface and electronic properties. Recently, different modification strategies have been employed for the construction of highly efficient CO_2 reduction reaction systems. Tang et al. developed a graphdiyne-decorated bismuth subcarbonate (marked as BOC@GDY) catalyst for CO_2 electrochemical reduction (Figure 5) [44]. The electron-rich nature of GDY can reduce the reduction potential of Bi(III) to Bi(0) , allowing more active sites for CO_2 reduction. Relative to bulk BOC and BOC, the smaller Tafel slope and Nyquist plot of BOC@GDY

indicated that a smaller charge transfer resistance and faster reaction kinetics were realized. The electrochemical CO₂ reduction results in Figure 5g revealed that BOC@GDY had a high formate selectivity (>91%) over a wide potential window of −0.65 to −1.1 V vs. reversible hydrogen electrode (RHE). Zhao et al. reported a surface reconstruction phenomenon on defect-rich ultrathin palladium nanosheets (donated as Pd NSs) during an aqueous CO₂ electrochemical reduction reaction [45]. A series of Pd NSs with different sizes in diagonal length (20, 50, and 120 nm) were studied. Interestingly, hexagonal Pd NSs with dominant (111) facet transformed into an irregular, wrinkled structure, accompanying by more exposed (100) facet. The resulting structural transformation increased the surface density of active sites and reduced the CO binding strength on the Pd surface, boosting the yield of CO from CO₂ electroreduction. In addition, loading isolated metal atoms on the ultrathin nanosheets was also an effective method for the improvement of CO₂ reduction activity due to the high metal utilization and numerous catalytically active sites. Si et al. employed a complex-exchange strategy to successfully anchor Au single atoms to ultrathin ZnIn₂S₄ nanosheets (Au/ZnIn₂S₄), enabling the precise tuning of CH₄ yield and selectively [46]. Relative to Au nanoparticles, Au single atoms possess abundant low-coordinated sites, which is beneficial for the adsorption and activation of CO₂ molecules, interfacial charge transfer, as well as the inhibition of the intermediate *CO desorption and stabilization of intermediate *CH₃ (Figure 6). Under visible light irradiation ($\lambda > 420$ nm), Au/ZnIn₂S₄ catalyst showed that the yield of CH₄ was 275 $\mu\text{mol g}^{-1} \text{h}^{-1}$, and selectivity was up to 77%. These above studies demonstrated that 2D ultrathin nanomaterials were an effective alternative for building the highly efficient CO₂ reduction systems.

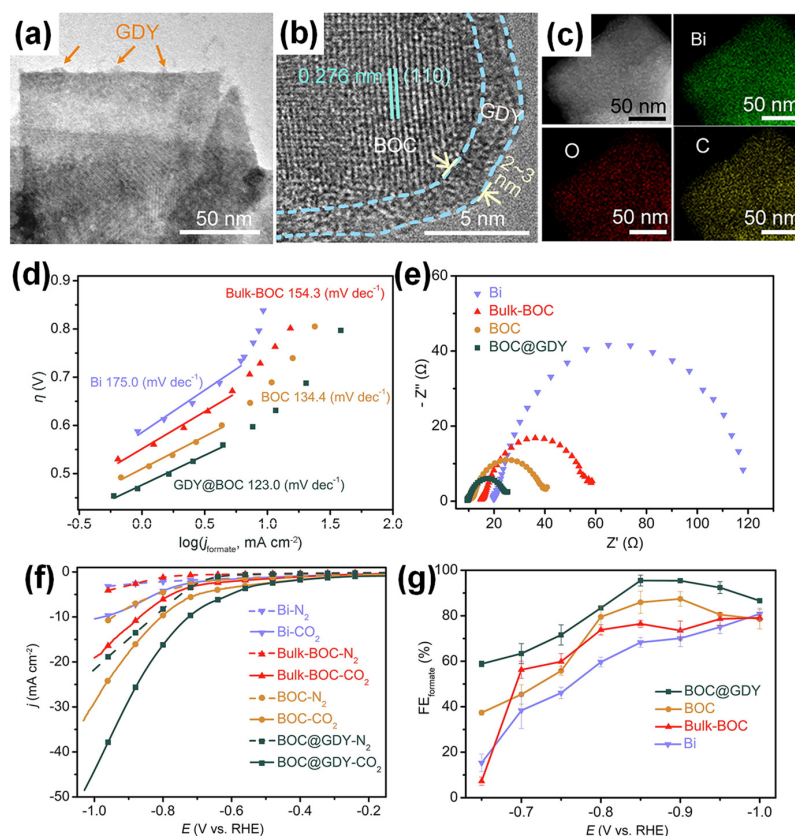


Figure 5. (a) TEM, (b) HRTEM, and (c) HAADF-STEM and element mapping images for BOC@GDY. Study for the influence of GDY and the catalytic mechanism of BOC@GDY for ECR. (d) Tafel plots and (e) Nyquist plots at −0.45 V vs. RHE for commercial Bi, bulk-BOC, BOC, and BOC@GDY in H-type cell; (f) LSV curves for commercial Bi, bulk-BOC, BOC and BOC@GDY; (g) FEs for formate over commercial Bi, bulk-BOC, BOC, and BOC@GDY [44]. Copyright 2021, Elsevier.

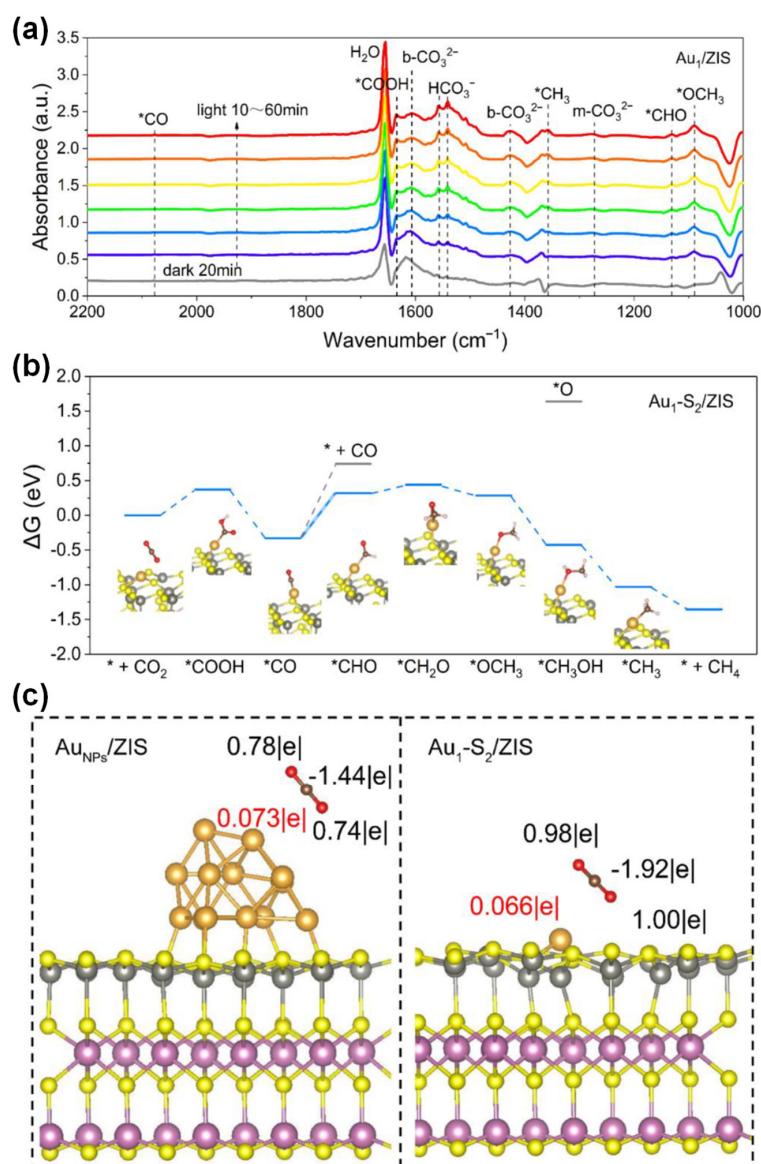


Figure 6. (a) In-situ DRIFTS for dynamic observation on the reaction intermediates during photocatalytic CO₂ reduction over Au/ZnIn₂S₄; (b) Free energy diagrams of photocatalytic CO₂ to CH₄ for Au/ZnIn₂S₄; (c) Optimized adsorption configurations of CO₂ molecules with their corresponding charge distribution on the surface of AuNPs/ZnIn₂S₄ and Au/ZnIn₂S₄ [46]. Copyright 2022, Wiley-VCH.

Ammonia, an essential component of the global economy, is widely used for the synthesis of crucial chemicals, including nitrogen fertilizer, pharmaceuticals, synthetics, etc. Moreover, ammonia is one of the great potential carriers for green hydrogen storage due to its high energy density, safety, and being non-flammable. It is also easy to liquefy storage. However, due to the extremely stable N≡N bonds, industrial ammonia production remains heavily reliant on the harsh Haber-Bosch process, which requires high temperature and high pressure. It is critical and urgent to develop alternative pathways for artificial dinitrogen fixation using photo/electrocatalysis under atmospheric pressure. Zhao et al. demonstrated a simple co-precipitation method for the preparation of M^{II}M^{III}-LDH (M^{II} = Mg, Zn, Ni, Cu; M^{III} = Al, Cr) nanosheet photocatalysts with oxygen vacancies and their successful application in photocatalytic nitrogen reduction at ambient temperature and pressure [47]. In the presence of pure water, the CuCr-LDH ultrathin nanosheet exhibited an extraordinarily high ammonia yield under visible light irradiation. Positron

annihilation spectroscopy and X-ray absorption fine structure measurements revealed that oxygen vacancies induced the distortions in the MO_6 octahedra of the LDH ultrathin nanosheets, advancing the improved photocatalytic performance. Density functional theory (DFT) calculations further clarified the structure-activity relationship in the CuCr-LDH system in terms of oxygen vacancies doping and compressive strain. A newly created defect level from the unoccupied Cr 3D orbitals likely served as electron-trapping sites to facilitate electron transfer from LDH to nitrogen. In addition, the electronic structures of CuCr-LDHs with and without defects were quite different for their mutative surface composition and structure, which in turn changed their adsorption energy for nitrogen on the surface of defect-free CuCr-pure, CuCr- V_O and CuCr- V_O -Strain (V_O defined as oxygen vacancies). The existence of oxygen vacancies and strained bonding in CuCr-LDH synergistically modulated the bandgap structure and charge transfer behavior, boosting the nitrogen photoreduction activity. For the investigation of dinitrogen electroreduction, molybdenum carbide (Mo_2C) nanodots embedded in ultrathin carbon nanosheets were successfully synthesized via a molten salt method. According to the experiments and DFT calculation results, Cheng et al. considered the increased ammonia yield was mainly derived from the unique electronic structure and abundant nitrogen adsorption active sites of Mo_2C nanodots, strengthening the cleavage of the nitrogen-nitrogen triple bond and hydrogenation (Figure 7) [48]. Moreover, a possible evolution path for ammonia synthesis on Mo_2C nanodots was also proposed.

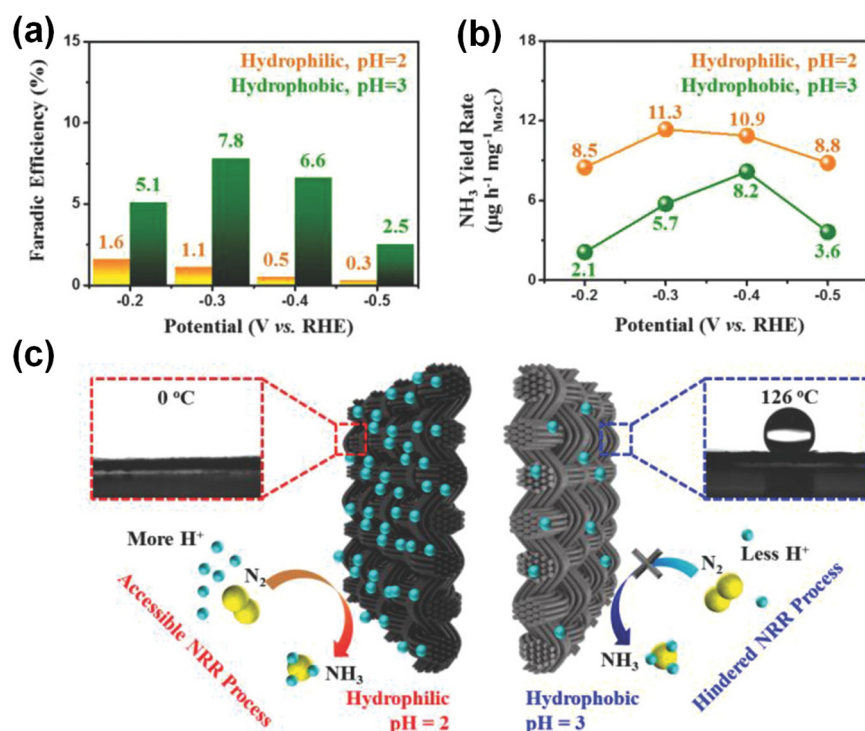


Figure 7. (a) Fes for ammonia and (b) corresponding yield rate over $\text{Mo}_2\text{C}/\text{C}$ catalyst. (c) Nitrogen reduction mechanism of the $\text{Mo}_2\text{C}/\text{C}$ under proton-suppressed and proton-enriched conditions, respectively [48]. Copyright 2018, Wiley-VCH.

Hydrogen is a credible candidate for the replacement of fossil fuels and energy feedstock for fuel cells. It is desirable to develop sustainable routes, such as electrocatalytic or photocatalytic processes to produce hydrogen. Among various 2D materials, graphitic carbon nitride ($\text{g-C}_3\text{N}_4$) material is regarded as a promising catalyst both for photochemical and electrochemical hydrogen evolution reactions owing to its good light absorption, suitable energy band structure, easily tunable structure, and high nitrogen content. In 2009, Wang et al. first applied $\text{g-C}_3\text{N}_4$ materials in the research of photo-splitting water for

hydrogen production [49]. Since then, a research boom in carbon nitride has been launched. Jin et al. fabricated an efficient 2D/2D $g\text{-C}_3\text{N}_4$ and molybdenum nitride ($g\text{-C}_3\text{N}_4\text{/MoN}$) heterojunction electrocatalyst via an interface engineering strategy for the alkaline hydrogen evolution reaction [50]. The formation of dual active sites in $g\text{-C}_3\text{N}_4\text{/MoN}$ profited by the unique hybrid structure is relevant to the enhanced electrocatalytic hydrogen evolution performance, in which N sites from $g\text{-C}_3\text{N}_4$ expedited H_{ad} adsorption and Mo atoms from MoN expedited OH_{ad} adsorption, respectively. Furthermore, combining metal oxide, metal sulfide, and phosphide materials with $g\text{-C}_3\text{N}_4$ ultrathin nanosheets to form heterojunction is also a valid approach for constructing highly efficient energy conversion systems [51–53]. Besides, Cao and co-workers synthesized WSe_2 monolayer nanosheets with intrinsic Se vacancies using a mechanical exfoliation method, followed by annealing treatment under different reaction temperatures [54]. The absent Se atoms enabled more exposed basal planes, enhancing the stabilization of hydrogen atoms on exposed W atoms. In order to broaden the application of BiOX materials in photocatalytic hydrogen evolution reactions, a bismuth-rich strategy was employed to modulate the electronic structure of BiOCl ultrathin nanosheets [55]. A bilayer junction was then established between monolayer MoS_2 and monolayer $\text{Bi}_{12}\text{O}_{17}\text{Cl}_2$ to provide the hydrogen evolution sites (Figure 8a). Simultaneously, a directional and efficient photogenerated electrons transfer was achieved via the formed interfacial Bi-S bonds in $\text{MoS}_2\text{/Bi}_{12}\text{O}_{17}\text{Cl}_2$. $\text{MoS}_2\text{/Bi}_{12}\text{O}_{17}\text{Cl}_2$ bilayer junction photocatalyst exhibited an unprecedented hydrogen evolution rate of $33\text{ mmol h}^{-1}\text{ g}^{-1}$ under visible light irradiation, as shown in Figure 8b.

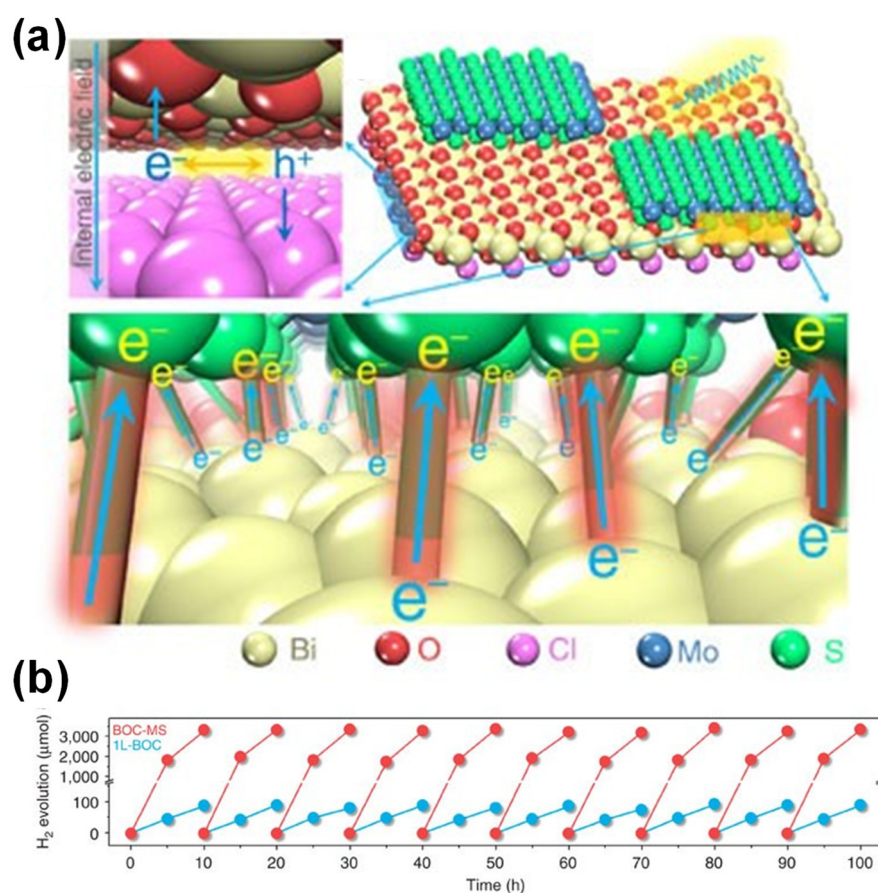


Figure 8. (a) Schematic illustration of the charge flow processes within monolayer MoS_2 and monolayer $\text{Bi}_{12}\text{O}_{17}\text{Cl}_2$, and the interfacial electron transfer along the Bi-S bonds of $\text{MoS}_2\text{/Bi}_{12}\text{O}_{17}\text{Cl}_2$ bilayer junction photocatalyst; (b) Cycling tests of photocatalytic H_2 evolution over as-prepared $\text{MoS}_2\text{/Bi}_{12}\text{O}_{17}\text{Cl}_2$ catalysts [55]. Copyright 2016, Nature Publishing Group.

4. Summary and Prospects

Developing highly efficient and cost-effective energy conversion systems is a critical component for advancing energy transformation and building a safe, green, and sustainable energy system. Recently, 2D ultrathin nanomaterials have been regarded as one of the most promising candidates for sustainable energy production due to their easily modulated components and electronic structures, even the outstanding performance in energy and environment researches. In this review, we have summarized the steerable fabrication of 2D ultrathin nanomaterials through the two main approaches, top-down and bottom-up. Moreover, the activity optimization strategies for the energy-related photo/electrochemical applications were also discussed, including surface vacancy engineering, single atoms loading, alloying, heterojunction construction, surface reconstruction, element doping, etc. Despite the breakthrough progress, there are several unexplored aspects still need to be studied, which will have significant scope in future.

A major challenge for the scale-up of ultrathin nanomaterials for industrial applications is the inability to achieve large-scale production with a highly controllable layer thickness. The corresponding methods need to be improved to realize the manufacture and storage of the nanomaterials with an ultrathin structure. The long-term stability and durability of the catalysts is another core issue that limits practical applications. In addition, with regard to photocatalysis, the ultrathin nanomaterials tend to agglomerate due to the presence of a loose powder during the reaction. Immobilizing the nanomaterials onto suitable substrates, like nickel foam and carbon fiber paper, offers a promising way to substantially increase ease of use. Moreover, theoretical understanding of the catalytic mechanisms in 2D ultrathin nanomaterials is still superficial and unclear, especially for CO₂ reduction and dinitrogen fixation systems. Current established model structures are still not clear to clarify the adsorption and activation of the substrate molecules, multi-electron transfer process, evolution of intermediates, as well as the dissociation products. Therefore, more fundamental and deep insight into catalytic mechanism are highly desired to distinctly reveal the structure-activity relationships in different catalytic systems.

Author Contributions: Writing—original draft preparation, F.L.; writing—review and editing, C.W.; resources and supervision, M.Z.; conceptualization, writing—review and editing, resources, and supervision, M.J. All authors have read and agreed to the published version of the manuscript.

Funding: This research was funded by [National Natural Science Foundation of China] grant number [22108108], [Jiangsu Province Higher Vocational Colleges Teacher Professional Leader High-end Research and Study Project, China] grant number [2022TDGDYX002].

Conflicts of Interest: The authors declare no conflict of interest.

References

1. Hisatomi, T.; Kubota, J.; Domen, K. Recent advances in semiconductors for photocatalytic and photoelectrochemical water splitting. *Chem. Soc. Rev.* **2014**, *43*, 752–7535. [[CrossRef](#)]
2. Hu, H.; Li, Q.; Li, L.Q.; Teng, X.L.; Feng, Z.X.; Zhang, Y.L.; Wu, M.B.; Qiu, J.S. Laser irradiation of electrode materials for energy storage and conversion. *Matter* **2020**, *3*, 95–126. [[CrossRef](#)]
3. Kibsgaard, J.; Chorkendorff, I. Considerations for the scaling-up of water splitting catalysts. *Nat. Energy* **2019**, *4*, 430–433. [[CrossRef](#)]
4. Prabhu, P.; Jose, V.; Lee, J.M. Heterostructured catalysts for electrocatalytic and photocatalytic carbon dioxide reduction. *Adv. Funct. Mater.* **2020**, *30*, 1910768. [[CrossRef](#)]
5. Arico, A.S.; Bruce, P.; Scrosati, B.; Tarascon, J.M.; Schalkwijk, W.V. Nanostructured materials for advanced energy conversion and storage devices. *Nat. Mater.* **2005**, *4*, 366–377. [[CrossRef](#)]
6. Hou, Y.X.; Lv, J.Q.; Quan, W.W.; Lin, Y.B.; Hong, Z.S.; Huang, Y.Y. Strategies for Electrochemically Sustainable H₂ Production in Acid. *Adv. Sci.* **2022**, *9*, 2104916. [[CrossRef](#)]
7. Li, L.Q.; Tang, C.; Jin, H.Y.; Davey, K.; Qiao, S.-Z. Main-group elements boost electrochemical nitrogen fixation. *Chem* **2021**, *7*, 3232–3255. [[CrossRef](#)]
8. Zhang, K.; Zhang, G.; Qu, J.H.; Liu, H.J. Disorder the atomic structure of Co(II) oxide via B-doping: An efficient oxygen vacancy introduction approach for high oxygen evolution reaction electrocatalysts. *Small* **2018**, *14*, 1802760. [[CrossRef](#)]

9. Novoselov, K.S.; Geim, A.K.; Morozov, S.V.; Jiang, D.; Zhang, Y.; Dubonos, S.V.; Grigorieva, I.V.; Firsov, A.A. Electric field effect in atomically thin carbon films. *Science* **2004**, *306*, 666–669. [[CrossRef](#)]
10. Xie, J.F.; Zhang, H.; Li, S.; Wang, R.X.; Sun, X.; Zhou, M.; Zhou, J.F.; Lou, X.W.; Xie, Y. Defect-rich MoS₂ ultrathin nanosheets with additional active edge sites for enhanced electrocatalytic hydrogen evolution. *Adv. Mater.* **2013**, *25*, 5807–5813. [[CrossRef](#)]
11. Chen, F.; Ma, T.Y.; Zhang, T.R.; Zhang, Y.H.; Huang, H.W. Atomic-level charge separation strategies in semiconductor-based photocatalysts. *Adv. Mater.* **2021**, *33*, 2005256. [[CrossRef](#)] [[PubMed](#)]
12. Ye, L.; Gao, Y.; Cao, S.Y.; Chen, H.; Yao, Y.; Hou, J.G.; Sun, L.C. Assembly of highly efficient photocatalytic CO₂ conversion systems with ultrathin two-dimensional metal–organic framework nanosheets. *Appl. Catal. B* **2018**, *227*, 54–60. [[CrossRef](#)]
13. Li, L.Y.; Xia, Y.B.; Zeng, M.Q.; Fu, L. Facet engineering of ultrathin two-dimensional materials. *Chem. Soc. Rev.* **2022**, *51*, 7327–7343. [[CrossRef](#)] [[PubMed](#)]
14. Sun, Y.F.; Gao, S.; Lei, F.C.; Xie, Y. Atomically-thin two-dimensional sheets for understanding active sites in catalysis. *Chem. Soc. Rev.* **2015**, *44*, 623–636. [[CrossRef](#)] [[PubMed](#)]
15. Wang, Y.; Mao, J.; Meng, X.G.; Yu, L.; Deng, D.H.; Bao, X.H. Catalysis with Two-Dimensional Materials Confining Single Atoms: Concept, Design, and Applications. *Chem. Rev.* **2019**, *119*, 1806–1854. [[CrossRef](#)] [[PubMed](#)]
16. Cao, S.W.; Shen, B.J.; Tong, T.; Fu, J.W.; Yu, J.G. 2D/2D Heterojunction of Ultrathin MXene/Bi₂WO₆ Nanosheets for Improved Photocatalytic CO₂ Reduction. *Adv. Funct. Mater.* **2018**, *28*, 1800136. [[CrossRef](#)]
17. Huang, N.; Wang, P.; Jiang, D. Covalent organic frameworks: A materials platform for structural and functional designs. *Nat. Rev. Mater.* **2016**, *1*, 16068. [[CrossRef](#)]
18. Zhang, J.; Vukmirovic, M.B.; Xu, Y.; Mavrikakis, M.; Adzic, R.R. Controlling the catalytic activity of platinum-monolayer electrocatalysts for oxygen reduction with different substrates. *Angew. Chem. Int. Ed.* **2005**, *44*, 2132–2135. [[CrossRef](#)]
19. Sahoo, D.P.; Das, K.K.; Mansingh, S.; Sultana, S.; Parida, K. Recent progress in first row transition metal Layered double hydroxide (LDH) based electrocatalysts towards water splitting: A review with insights on synthesis. *Coord. Chem. Rev.* **2022**, *469*, 214666. [[CrossRef](#)]
20. Han, Q.; Bai, X.; Man, Z.; He, H.; Li, L.; Hu, J.; Alsaedi, A.; Hayat, T.; Yu, Z.; Zhang, W.; et al. Convincing synthesis of atomically thin, single-crystalline InVO₄ sheets toward promoting highly selective and efficient solar conversion of CO₂ into CO. *J. Am. Chem. Soc.* **2019**, *141*, 4209. [[CrossRef](#)]
21. Pandey, M.; Jacobsen, K.W.; Thygesen, K.S. Atomically thin ordered alloys of transition metal dichalcogenides: Stability and band structures. *J. Phys. Chem. C* **2016**, *120*, 23024–23029. [[CrossRef](#)]
22. Zhou, J.D.; Zeng, Q.S.; Lv, D.H.; Sun, L.F.; Niu, L.; Fu, W.; Liu, F.C.; Shen, Z.X.; Jin, C.H.; Liu, Z. Controlled Synthesis of High-Quality Monolayered α -In₂Se₃ via Physical Vapor Deposition. *Nano Lett.* **2015**, *15*, 6400–6405. [[CrossRef](#)] [[PubMed](#)]
23. Zhou, Y.Q.; Tao, L.; Chen, Z.F.; Lai, H.J.; Xie, W.G.; Xu, J.B. Defect Etching of Phase-Transition-Assisted CVD-Grown 2H-MoTe₂. *Small* **2021**, *17*, 2102146. [[CrossRef](#)] [[PubMed](#)]
24. Chen, J.L.; Wang, G.Y.; Tang, Y.N.; Tian, H.; Xu, J.P.; Dai, X.Q.; Xu, H.; Jia, J.F.; Ho, W.; Xie, M.H. Quantum Effects and Phase Tuning in Epitaxial Hexagonal and Monoclinic MoTe₂ Monolayers. *ACS Nano* **2017**, *11*, 3282–3288. [[CrossRef](#)] [[PubMed](#)]
25. Zheng, W.; Feng, W.; Zhang, X.; Chen, X.S.; Liu, G.B.; Qiu, Y.F.; Hasan, T.; Tan, P.H.; Hu, P.A. Anisotropic Growth of Nonlayered CdS on MoS₂ Monolayer for Functional Vertical Heterostructures. *Adv. Funct. Mater.* **2016**, *26*, 2648–2654. [[CrossRef](#)]
26. Lukowski, M.A.; Daniel, A.S.; English, C.R.; Meng, F.; Forticaux, A.; Hamers, R.J.; Jin, S. Highly Active Hydrogen Evolution Catalysis from Metallic WS₂ Nanosheets. *Energy Environ. Sci.* **2014**, *7*, 2608–2613. [[CrossRef](#)]
27. Yang, S.B.; Gong, Y.J.; Zhang, J.S.; Zhan, L.; Ma, L.L.; Fang, Z.Y.; Vajtai, R.; Wang, X.C.; Ajayan, P.M. Exfoliated Graphitic Carbon Nitride Nanosheets as Efficient Catalysts for Hydrogen Evolution Under Visible Light. *Adv. Mater.* **2013**, *25*, 2452–2456. [[CrossRef](#)]
28. Zhu, W.S.; Gao, X.; Li, Q.; Li, H.P.; Chao, Y.H.; Li, M.J.; Mahurin, S.M.; Li, H.M.; Zhu, H.Y.; Dai, S. Controlled gas exfoliation of boron nitride into few-layered nanosheets. *Angew. Chem. Int. Ed.* **2016**, *55*, 10766–10770. [[CrossRef](#)]
29. Zheng, Y.J.; Zhou, H.X.; Liu, D.; Floudas, G.; Wagner, M.; Koynov, K.; Mezger, M.; Butt, H.J.; Ikeda, T. Supramolecular Thiophene Nanosheets. *Angew. Chem. Int. Ed.* **2013**, *52*, 4845–4848. [[CrossRef](#)]
30. Ji, M.X.; Di, J.; Zhao, J.Z.; Chen, C.; Zhang, Y.; Liu, Z.H.; Li, H.P.; Xia, J.X.; He, M.Q.; Li, H.M. Orientated dominating charge separation via crystal facet homojunction inserted into BiOBr for solar-driven CO₂ conversion. *J. CO₂ Util.* **2022**, *59*, 101957. [[CrossRef](#)]
31. Zhou, Y.E.; Zhang, L.Y.; Lin, L.H.; Wygant, B.R.; Liu, Y.; Zhu, Y.; Zheng, Y.B.; Mullins, C.B.; Zhao, Y.; Zhang, X.H.; et al. Highly Efficient Photoelectrochemical Water Splitting from Hierarchical WO₃/BiVO₄ Nanoporous Sphere Arrays. *Nano Lett.* **2017**, *17*, 8012–8017. [[CrossRef](#)] [[PubMed](#)]
32. Ji, M.X.; Shao, Y.F.; Nkudede, E.; Liu, Z.H.; Sun, X.; Zhao, J.Z.; Chen, Z.R.; Yin, S.; Li, H.M.; Xia, J.X. Oxygen vacancy triggering the broad-spectrum photocatalysis of bismuth oxyhalide solid solution for ciprofloxacin removal. *J. Colloid Interface Sci.* **2022**, *626*, 221–230. [[CrossRef](#)] [[PubMed](#)]
33. Cheng, W.R.; He, J.F.; Yao, T.; Sun, Z.H.; Jiang, Y.; Liu, Q.H.; Jiang, S.; Hu, F.C.; Xie, Z.; He, B.; et al. Half-Unit-Cell α -Fe₂O₃ Semiconductor Nanosheets with Intrinsic and Robust Ferromagnetism. *J. Am. Chem. Soc.* **2014**, *136*, 10393–10398. [[CrossRef](#)] [[PubMed](#)]
34. Zhou, Y.G.; Zhang, Y.F.; Lin, M.S.; Long, J.L.; Zhang, Z.Z.; Lin, H.X.; Wu, J.C.S.; Wang, X.X. Monolayered Bi₂WO₆ nanosheets mimicking heterojunction interface with open surfaces for photocatalysis. *Nat. Commun.* **2015**, *6*, 8340. [[CrossRef](#)]

35. Di, J.; Xia, J.X.; Ji, M.X.; Xu, L.; Yin, S.; Chen, Z.G.; Li, H.M. Bidirectional acceleration of carrier separation spatially via N-CQDs/atomically-thin BiOI nanosheets nanojunctions for manipulating active species in a photocatalytic process. *J. Mater. Chem. A* **2016**, *4*, 5051–5061. [[CrossRef](#)]
36. Ji, M.X.; Xia, J.X.; Di, J.; Liu, Y.L.; Chen, R.; Chen, Z.G.; Yin, S.; Li, H.M. Graphene-like boron nitride induced accelerated charge transfer for boosting the photocatalytic behavior of Bi₄O₅I₂ towards bisphenol a removal. *Chem. Eng. J.* **2018**, *331*, 355–363. [[CrossRef](#)]
37. Wang, B.; Yang, S.Z.; Chen, H.L.; Gao, Q.; Weng, Y.X.; Zhu, W.S.; Liu, G.P.; Zhang, Y.; Ye, Y.Z.; Zhu, H.Y.; et al. Revealing the role of oxygen vacancies in bimetallic PbBiO₂Br atomic layers for boosting photocatalytic CO₂ conversion. *Appl. Catal. B* **2020**, *277*, 119170. [[CrossRef](#)]
38. Di, J.; Chen, C.; Zhu, C.; Song, P.; Xiong, J.; Ji, M.X.; Zhou, J.D.; Fu, Q.D.; Xu, M.Z.; Hao, W.; et al. Bismuth Vacancy-Tuned Bismuth Oxybromide Ultrathin Nanosheets toward Photocatalytic CO₂ Reduction. *ACS Appl. Mater. Interfaces* **2019**, *11*, 30786–30792. [[CrossRef](#)]
39. Han, S.G.; Ma, D.D.; Zhou, S.H.; Zhang, K.X.; Wei, W.B.; Du, Y.H.; Wu, X.T.; Xu, Q.; Zou, R.Q.; Zhu, Q.L. Fluorine-tuned single-atom catalysts with dense surface Ni-N₄ sites on ultrathin carbon nanosheets for efficient CO₂ electroreduction. *Appl. Catal. B* **2021**, *283*, 119591. [[CrossRef](#)]
40. Zhang, G.G.; Zhang, M.W.; Ye, X.X.; Qiu, X.Q.; Lin, S.; Wang, X.C. Iodine Modified Carbon Nitride Semiconductors as Visible Light Photocatalysts for Hydrogen Evolution. *Adv. Mater.* **2014**, *26*, 805–809. [[CrossRef](#)]
41. Liu, Y.W.; Hua, X.M.; Xiao, C.; Zhou, T.F.; Huang, P.C.; Guo, Z.P.; Pan, B.C.; Xie, Y. Heterogeneous Spin States in Ultrathin Nanosheets Induce Subtle Lattice Distortion To Trigger Efficient Hydrogen Evolution. *J. Am. Chem. Soc.* **2016**, *138*, 5087–5092. [[CrossRef](#)] [[PubMed](#)]
42. Ji, M.X.; Zhang, Z.Y.; Xia, J.X.; Di, J.; Liu, Y.L.; Chen, R.; Yin, S.; Zhang, S.; Li, H.M. Enhanced photocatalytic performance of carbon quantum dots/BiOBr composite and mechanism investigation. *Chin. Chem. Lett.* **2018**, *29*, 805–810.
43. Maeda, K.; Eguchi, M.; Oshima, T. Perovskite oxide nanosheets with tunable band-edge potentials and high photocatalytic hydrogen-evolution activity. *Angew. Chem. Int. Ed.* **2014**, *53*, 13164–13168. [[CrossRef](#)]
44. Tang, S.F.; Lu, X.L.; Zhang, C.; Wei, Z.W.; Si, R.; Lu, T.B. Decorating graphdiyne on ultrathin bismuth subcarbonate nanosheets to promote CO₂ electroreduction to formate. *Sci. Bull.* **2021**, *66*, 1533–1541. [[CrossRef](#)]
45. Zhao, Y.; Tan, X.; Yang, W.F.; Jia, C.; Chen, X.J.; Ren, W.H.; Smith, S.C.; Zhao, C. Surface Reconstruction of Ultrathin Palladium Nanosheets during Electrocatalytic CO₂ Reduction. *Angew. Chem. Int. Ed.* **2020**, *59*, 21493–21498. [[CrossRef](#)] [[PubMed](#)]
46. Si, S.H.; Shou, H.W.; Mao, Y.Y.; Bao, X.L.; Zhai, G.Y.; Song, K.P.; Wang, Z.Y.; Wang, P.; Liu, Y.Y.; Zheng, Z.K.; et al. Low-Coordination Single Au Atoms on Ultrathin ZnIn₂S₄ Nanosheets for Selective Photocatalytic CO₂ Reduction towards CH₄. *Angew. Chem. Int. Ed.* **2022**, *61*, e202209446. [[CrossRef](#)] [[PubMed](#)]
47. Zhao, Y.F.; Zhao, Y.X.; Waterhouse, G.I.N.; Zheng, L.R.; Cao, X.Z.; Teng, F.; Wu, L.Z.; Tung, C.H.; O'Hare, D.; Zhang, T.R. Layered-Double-Hydroxide Nanosheets as Efficient Visible-Light-Driven Photocatalysts for Dinitrogen Fixation. *Adv. Mater.* **2017**, *29*, 1703828. [[CrossRef](#)]
48. Cheng, H.; Ding, L.X.; Chen, G.F.; Zhang, L.L.; Xue, J.; Wang, H.H. Molybdenum Carbide Nanodots Enable Efficient Electrocatalytic Nitrogen Fixation under Ambient Conditions. *Adv. Mater.* **2018**, *30*, 1803694. [[CrossRef](#)]
49. Wang, X.C.; Maeda, K.; Thomas, A.; Takanabe, K.; Xin, G.; Carlsson, J.M.; Domen, K.; Antonietti, M. A metal-free polymeric photocatalyst for hydrogen production from water under visible light. *Nat. Mater.* **2009**, *8*, 76–80. [[CrossRef](#)]
50. Jin, H.Y.; Liu, X.; Jiao, Y.; Vasileff, A.; Zheng, Y.; Qiao, S.Z. Constructing tunable dual active sites on two-dimensional C₃N₄@MoN hybrid for electrocatalytic hydrogen evolution. *Nano Energy* **2018**, *53*, 690–697. [[CrossRef](#)]
51. Hou, Y.D.; Laursen, A.B.; Zhang, J.S.; Zhang, G.G.; Zhu, Y.S.; Wang, X.C.; Dahl, S.; Chorkendorff, I. Layered Nanojunctions for Hydrogen-Evolution Catalysis. *Angew. Chem. Int. Ed.* **2013**, *52*, 3621–3625. [[CrossRef](#)]
52. Wang, Y.H.; Liu, L.Z.; Ma, T.Y.; Zhang, Y.H.; Huang, H.W. 2D Graphitic Carbon Nitride for Energy Conversion and Storage. *Adv. Funct. Mater.* **2021**, *31*, 2102540. [[CrossRef](#)]
53. Tan, X.Q.; Ng, S.F.; Mohamed, A.R.; Ong, W.J. Point-to-face contact heterojunctions: Interfacial design of 0D nanomaterials on 2D g-C₃N₄ towards photocatalytic energy applications. *Carbon Energy* **2022**, *4*. [[CrossRef](#)]
54. Sun, Y.; Zhang, X.W.; Mao, B.G.; Cao, M.H. Controllable selenium vacancy engineering in basal planes of mechanically exfoliated WSe₂ monolayer nanosheets for efficient electrocatalytic hydrogen evolution. *Chem. Commun.* **2016**, *52*, 14266. [[CrossRef](#)] [[PubMed](#)]
55. Li, J.; Zhan, G.M.; Yu, Y.; Zhang, L.Z. Superior visible light hydrogen evolution of Janus bilayer junctions via atomic-level charge flow steering. *Nat. Commun.* **2016**, *7*, 11480. [[CrossRef](#)] [[PubMed](#)]